Wear 265 (2008) 1687–1699

Contents lists available at ScienceDirect

Wear

journal homepage: www.elsevier.com/locate/wear

Contact pressure evolution and its relation to wear in sheet metal forming

Michael P. Pereira [a,*], Wenyi Yan [b], Bernard F. Rolfe [c]

[a] *Centre for Material & Fibre Innovation, Deakin University, Geelong, VIC 3217, Australia*
[b] *Department of Mechanical & Aerospace Engineering, Monash University, Clayton, VIC 3800, Australia*
[c] *School of Engineering & Information Technology, Deakin University, Geelong, VIC 3217, Australia*

ARTICLE INFO

Article history:
Received 18 July 2007
Received in revised form 11 March 2008
Accepted 11 April 2008
Available online 2 July 2008

Keywords:
Contact pressure
Finite element analysis
Sheet metal forming
Wear

ABSTRACT

For a given sheet metal forming process, an accurate determination of the contact pressure distribution is an essential step towards the estimation of tool life. This investigation utilizes finite element (FE) analysis to model and explain the evolution and distribution of contact pressure over the die radius, throughout the duration of a channel forming process. It was found that a typical two-peak steady-state contact pressure response exists for the majority of the process. However, this was preceded by an initial transient response, characterized by extremely large and localized contact pressures, which were more than double the magnitude of the steady-state peak pressure. The validity of the predicted contact pressure behavior was assessed via detailed numerical analysis and by examining the wear response of an experimental stamping operation. The experimental results revealed that the high contact pressure zones of the transient response corresponded to a severe galling wear mechanism. Therefore, the transient response may be of primary significance to the tool wear response; thus questioning the applicability of traditional bending-under-tension wear tests for sheet metal stamping processes. Finally, a parametric study was conducted, examining the influence of the major process parameters on the steady-state and peak transient contact pressures, using the developed FE model. It was found that the bend ratio and the blank material ultimate tensile strength had the most influence on the peak contact pressures. The main process-related parameters, friction coefficient and blank holder force, were found to have only a minor influence.

1. Introduction

In recent years, the automotive sheet metal forming industry has seen the implementation of higher strength steels to meet crash requirements, the reduced use of lubricants owing to environmental concerns, and the need for increased tool life due to the development of common vehicle platforms. Consequently, forming tools are now required to withstand higher forming forces for longer periods of time; leading to unacceptable levels of wear and galling. Wear problems can be costly due to the need for expensive wear resistant materials and coatings, increased stoppages and tool maintenance, and poor part quality in terms of surface finish and geometric accuracy. Hence, an accurate prediction of tool life has become an ever increasing requirement.

Unfortunately, wear is a complex systems response, and not simply an individual material property or unique physical mechanism [1]. As such, there are hundreds of equations in the literature to describe many types of wear [2]. Some of the empirical-based relationships in the literature, which describe both abrasive and adhesive surface wear in sliding contact, include those presented by Rhee [3], Bayer [4] and Archard [5]. In this type of equation, wear rate W is commonly expressed as a function of normal load L, sliding distance S (or sliding velocity and time), and wear coefficient K, in the following form:

$$W = KL^m S^n, \quad (1)$$

where m and n are empirical constants, fitted using data from simulative laboratory testing [6]. In general, it has been observed that $m \geq 1$ (with typical values in the range of 2–3) and $n \leq 1$ [1]. The power relationship between wear and normal load, where the exponent is greater than unity, suggests that the peak loads can have a significant influence on the wear response. This is in agreement with recent results presented by Yan et al.; where it was determined that the wear rate is very sensitive to the maximum contact pressure [7,8].

Therefore, a vital step towards the application of a suitable wear model is the accurate determination of the contact pressure, and the peak contact pressures in particular, at the sliding interface. For drawing-type processes, the die radius region of the tool is subjected to the most severe tribological stresses, as indicated by high wear levels typically seen in this vicinity. Hence, this paper

* Corresponding author. Tel.: +61 3 5227 3357; fax: +61 3 5227 1103.
E-mail address: mperei@deakin.edu.au (M.P. Pereira).

0043-1648/$ – see front matter © 2008 Elsevier B.V. All rights reserved.
doi:10.1016/j.wear.2008.04.042

investigates the magnitude and distribution of contact pressure over the die radius for a particular stamping process.

The novel contribution of this paper is to utilize FE analysis to examine the contact pressure evolution over the die radius for a typical channel forming process. In particular, a *transient* contact pressure response was identified, which has not been observed in previous studies of contact pressure/wear in sheet metal forming [9–13]. The identified transient conditions are speculated to be of primary significance to the wear response, due to large and localized contact pressures that are found to occur. This finding potentially questions the applicability of traditional wear tests for sheet metal stamping processes.

2. Experimental and numerical setup

The channel forming process shown in Fig. 1 was used to replicate the wear conditions experienced by a typical sheet metal stamping die in the automotive industry [14,15]. The stated references contain a detailed description of the semi-industrial wear test setup, procedure and results. The key variables are summarized in Table 1. The blank material used for this investigation is an uncoated 2.0 mm thick Dual Phase 600 grade steel (DP600). These process conditions (geometry, forming mode, blank material and thickness) were chosen as they are representative of typical auto-body structural components, such as rails, cross-members and pillars [14,16]. Such conditions are found to be prone to wear and galling [14].

The experimental process was replicated in the numerical simulation, using a non-linear implicit FE code (ABAQUS/Standard Version 6.5–1) [17]. The analysis was simplified to a one-half symmetric, two-dimensional plane-strain problem. In order to analyze the contact between the blank and die radius in detail, the die mesh and blank mesh were significantly refined in the region of the respective interfaces (Fig. 1c). Due to the simulation of contact and the significant bending experienced by the blank, four-node, bilinear, plane strain, quadrilateral elements with reduced integration point and enhanced hourglass control (CPE4R) were used to mesh all parts. A small number of three-node, linear, plane strain, triangular elements (CPE3) were used to allow the transition from a fine mesh in the region of the die radius, to a course mesh over the rest of the die. Tie constraints were used to merge together dissimilar regions of coarse and fine meshes, allowing faster transitions in mesh density near the interacting surfaces of interest (Fig. 1c). The use of tie constraints significantly reduced the number of elements required, resulting in a 75% reduction in computational time, with negligible affect on the predicted stresses, strains, forces and contact pressures throughout the model. Details of the FE mesh used are shown in Table 2. The side length of the elements at the interface between the blank and the die radius are also listed for reference.

The isotropic material properties of the blank and tools (die, punch, blank holder) are summarized in Table 3. Elasticity was included in the definition of the tool material to ensure that accu-

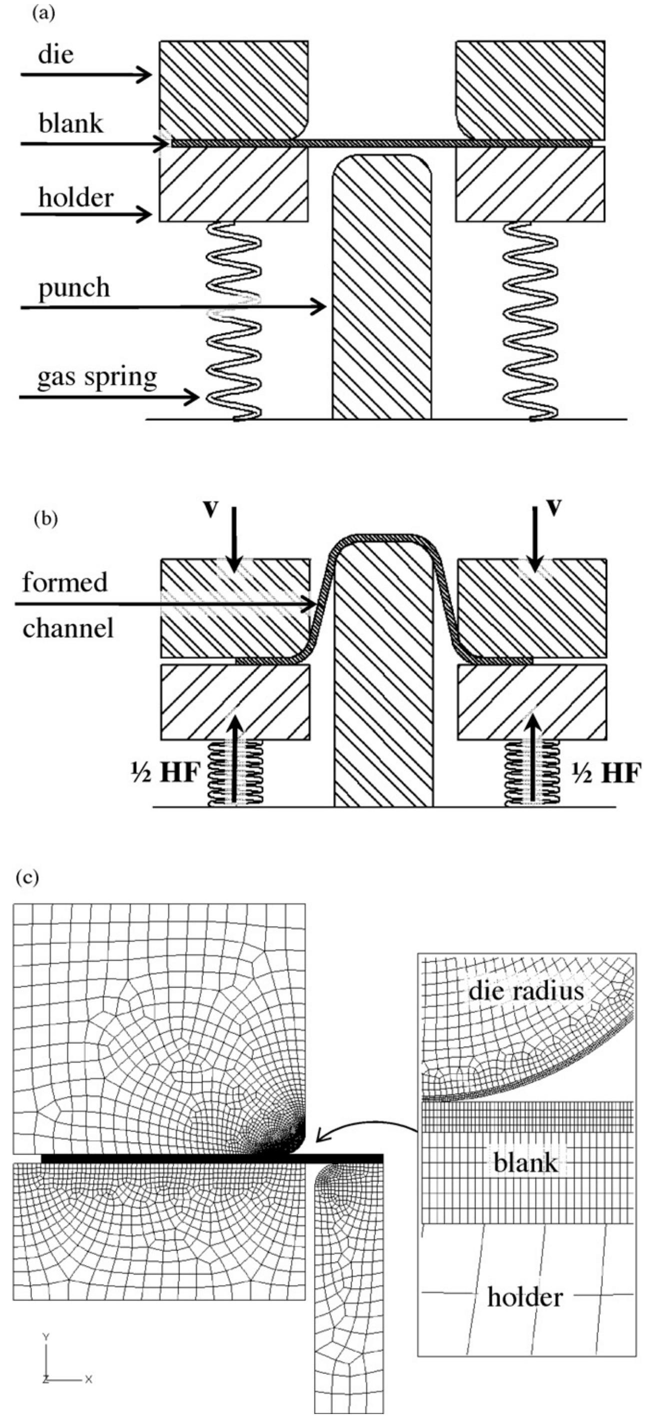

Fig. 1. Schematic of the channel forming wear test, (a) prior to the forming stroke and (b) at the end of the forming stroke. (c) FE model geometry, showing local mesh refinement near the blank–die radius interface.

Table 1
Summary of process variables for channel forming wear test

Press rate		55 min^{-1}
Punch width	a	30 mm
Draw depth	d	50 mm
Final flange length	f	11 mm
Die–to–punch gap	g	2.1 mm
Blank length	l	150 mm
Initial blank holder pressure	P_h	~8 MPa
Die radius	R_d	5 mm
Punch radius	R_p	5 mm
Blank thickness	t	2 mm
Blank width	w	25 mm
Tool-to-sheet clearance (= $t - g$)	c	0.1 mm

Table 2
Details of the FE mesh

No. of blank elements	8400
No. of die elements	3097
Total no. of CPE3 elements	20
Total no. of elements	12463
Min. blank element length @ interface	0.0625 mm
Min. die element length @ interface	0.0327 mm
Die–to–blank element length ratio @ interface	Approx 1:2

Table 3
Material properties of blank and tools

	Blank	Tools
Material definition	Elastic–plastic	Elastic
Elastic modulus (GPa)	205	205
Yield strength (MPa)	400	–
Tensile strength (MPa)	660	–
Strength coefficient, K	1016	–
Strain hardening index, n	0.15	–

rate contact pressures were predicted – as opposed to the rigid simplification commonly found in sheet metal forming FE analyses. For the DP600 blank material, it was found that the plastic behavior, measured during tensile tests, could be approximated well by a standard power law model (see Eq. (3) and Table 3 for the power law model and fitted parameters).

The interactions between the blank and tool surfaces were defined using the default 'master–slave' algorithm in ABAQUS, with a 'hard contact' pressure over-closure relationship [17]. Since the tools are significantly stiffer than the blank, the tool surfaces were set as the master surfaces in each of the contact interactions. Friction was modeled using an isotropic penalty friction formulation. The coefficient of friction was varied in order to correlate the experimentally measured flange length f and punch force with those predicted by the numerical simulation. Good correlation was achieved with a friction coefficient of 0.15. A constant blank holder force of 450 N was applied (equating to the 8 MPa initial contact pressure in the experimental setup).

3. Contact pressure prediction

Section 1 highlighted the significance of the contact pressure to the wear response. This section will examine the contact pressure behavior over the die radius, in terms of the overall distribution, the magnitude and location of peak stresses, and the evolution of these throughout the process.

3.1. Contact pressure distribution and evolution

Fig. 2 shows the predicted contact pressure distribution over the die radius at several instances during the simulation results history. For reference, the inset in each graph shows a three-dimensional representation of the deformed blank at the particular instant during the simulation. It is evident that the contact pressure response is complex, varying significantly over the die radius and throughout the forming process, and therefore cannot be completely captured in the five graphs presented in Fig. 2. To obtain a better understanding of the clearly time-dependent evolution of contact pressure it is necessary to plot the distributions at many more instances throughout the simulation results history. Such results were presented in earlier work by the authors via a three-dimensional surface plot, for a similar model/process setup [18], but this did not completely and plainly show the contact pressure response. To avoid the complexity of this three-dimensional graph, a contour plot of the contact pressure over the die radius vs. the punch stroke was created (Fig. 3). This type of graph permitted the illustration of the contact pressure distribution at many more instances in the results history (approximately 140 instances in this case), allowing a detailed and concise representation of the entire contact pressure response.

Due to the use of the strict master–slave contact formulation to model the die–blank interaction, the contact pressure results could only be reported at the blank (slave) surface, which was continually moving throughout the simulation. For this reason, the contact pressure data on the blank surface at each solution increment was translated and standardized to achieve a consistent location for the

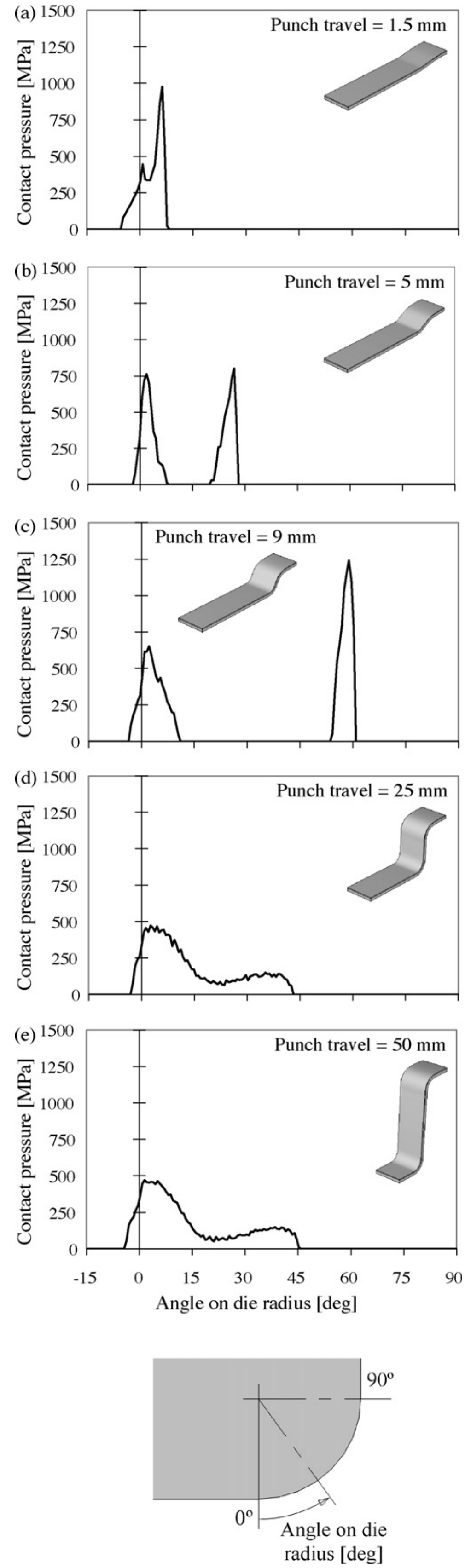

Fig. 2. Predicted contact pressure distribution over the die radius at five different instances during the simulation (insets show 3D representation of the deformed blank).

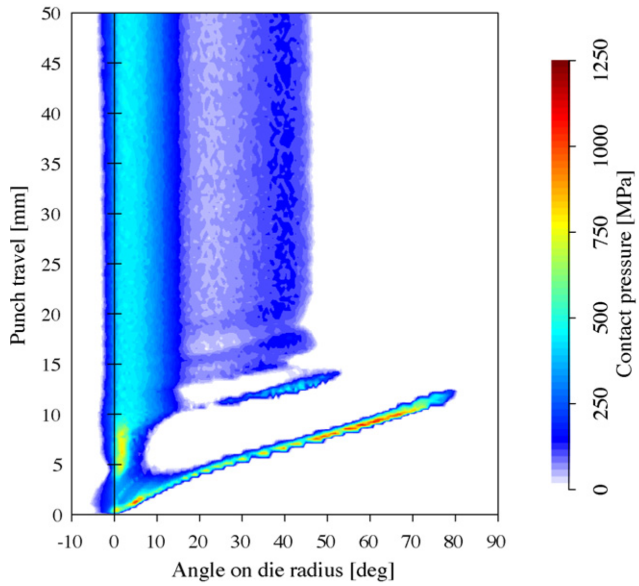

Fig. 3. Evolution of contact pressure over the die radius as the punch travels upwards.

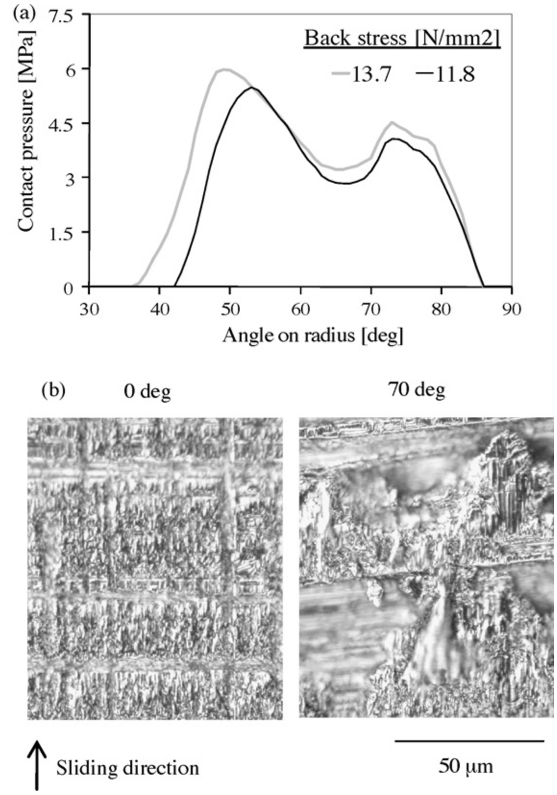

Fig. 4. (a) Experimentally measured pressure distribution over the radius of a bending-under-tension test for 0.8 mm thick mild steel strip drawn over a 20 mm radius at various back tensions (adapted from [12]). (b) Optical microscope images at two locations on die radius surface (after 140 parts were formed), from laboratory-based channel forming wear test.

angle on the die radius (at intervals of approximately 0.5° on the die radius). This procedure produced an array of contact pressure data at each interval of angle on radius vs. punch stroke.

The contact pressure distribution over the die radius at any instant during the simulation can be determined by examining Fig. 3. For example, to determine the contact pressure distribution when the punch has traveled 9 mm; the reader must follow a horizontal line, from left to right, at the 9 mm location along the vertical axis. Examining the regions where the line intersects the colored contours allows the pressure distribution along the radius to be determined. It is evident that there is a peak of approximately 500 MPa near 0° on the die radius, and another peak of approximately 1200 MPa close to 60°; resulting in the two-peak distribution shown in Fig. 2c.

Examination of Fig. 3 reveals that the contact pressure response can be divided into two distinct phases. Approximately two-thirds of the process, between 17 and 50 mm of punch travel, exhibits an almost constant contact pressure response – this will be referred to as the *steady-state* region. It is worth emphasizing that despite the relatively constant contact pressure distribution in this region, the blank still experiences significant deformation as it is continually drawn over the die radius, as illustrated by the deformation of the blank shown in Fig. 2. During the initial part of the process, between 0 and 17 mm of punch travel, the magnitude, location and distribution of contact pressure on the die radius varies considerably – this will consequently be referred to as the *transient* region. In order to understand and rationalize the predicted contact pressure response, the steady-state and transient contact pressure responses will be examined in further detail in the proceeding sub-sections.

3.2. Steady-state contact pressure distribution

The single contact pressure distribution obtained at the end of the simulation (i.e. Fig. 2e), will be chosen as representative of the steady-state response due to the approximately constant nature of this phase. In this graph, the contact pressure over the die radius shows two distributed peaks. The first peak occurs as the blank begins contact with the die radius, and the second (smaller) peak occurs where the blank leaves the die radius. The blank remains in contact with the die between these two peaks, with a pressure minimum at approximately the midpoint. It is also evident that contact between the blank and die (i.e. non-zero contact pressures) occurs over only approximately half of the radius during this steady-state stage of the process. Therefore, although the geometric angle of wrap of the blank is close to 90°, the actual angle of contact on the die radius is much less.

The characteristic two-peak contact pressure distribution described above qualitatively compares well with measured and predicted contact pressure distributions over the radii for other draw die forming processes presented in the literature [9–13]. For example, Fig. 4a shows results presented by Hanaki and Kato [12], which are contact pressure forces recorded from experimental bending-under-tension tests using mild steel at two prescribed values of back tension. Despite the different process under consideration, the contact pressure distributions in Fig. 4a exhibit qualitatively similar peaks at the beginning and end of contact and the pressure minima near the midpoint of the contact zone, as observed in Fig. 2e. The relative location of the contact pressure distribution for the bending-under-tension test differs to the channel forming process due to the differing geometry of the testing setup.

Hanaki and Kato [12] attribute the initial and secondary pressure peaks to the bending and unbending, respectively, that occurs as the sheet is continually drawn over the radius. Examination of the blank deformation during the channel forming simulation reveals that a similar drawing-type process occurs. For the most part, the initially straight blank is bent over the die radius to form a curvature. The blank is then drawn over this curvature, remaining largely in contact with the die radius, until it is straightened as it exits the radius. However, since the bending-under-tension test is a continuous-type process, it can be logically assumed that the transient response of the channel forming process will not be captured.

The qualitative agreement in results observed between the numerical and experimental results highlights that the bending-under-tension test provides similar contact conditions to the steady-state portion of the channel forming process. This agreement in results between the FE analysis and experiment methods, combined with the correlation between the recorded punch force and flange lengths described in Section 2, provides a reasonable level of confidence in the accuracy of the FE model.

3.3. Transient contact pressure response

The transient portion of the contact pressure evolution, denoted by the region between 0 mm and approximately 17 mm of punch travel, is dominated by highly localized contact conditions. These result in contact pressures exceeding 1000 MPa – i.e. more than double the steady-state peak pressures. The contact pressure contour (Fig. 3) shows that a local pressure maximum occurs at a region close to 0° on the radius for almost the entire process. However, during the transient stage this local maximum is, for the most part, exceeded by a second pressure peak further along the radius. The second peak is more localized, with an approximate area of contact between the blank and die of less than 10° (less than 0.9 mm arc length), in general. Furthermore, this pressure peak does not remain at the same location on the die radius, but instead moves along the radius at an almost constant rate with respect to the punch travel. Therefore, although the transient peak contact pressure is highly localized at any given instant during the simulation, these severe pressures are experienced over a large portion of the die radius during the process.

The varying contact pressure response during the transient region occurs as a result of the changing geometric, loading and contact conditions as the straight blank is initially wrapped/formed over the die radius by the action of the punch. Although the literature contains several investigations which have examined the contact pressure distributions over radii for drawing-type metal forming processes, using experimental and FE methods [9–13], this transient effect is not observed. The reason is that each of these investigations examined the drawing of sheet metal over a radius using various types of the bending-under-tension test, which is essentially a continuous/steady process.

In order to assess the validity of the transient contact pressure results, and the significance of the results with regard to the wear response, laboratory-based channel forming wear tests have been conducted. The geometry and blank material for this test are the same as those described in Section 2. The die material is an AISI D2 grade tool steel, hardened to 60 HRC. Optical microscope images at two locations on the die radius surface are shown in Fig. 4b, after 140 parts were formed. It is evident that an abrasive wear mechanism occurs at the location of 0° on the die radius, whilst a more severe galling mechanism is observed at the 70° location.

The results presented in Fig. 4b correlate well with the contact pressure results predicted over the die radius (Fig. 3). According to Fig. 3, the location of 0° on the die radius corresponds to moderate contact pressures (∼500 MPa), which result in the abrasive wear mechanism in observed in Fig. 4b. The region of 70° on the die radius corresponds to higher contact pressures (>1000 MPa), resulting in the transition to the more severe galling mechanism. The results from the experimental analysis show similar correlation between the contact pressure and the type/severity of the wear mechanism at all other locations on the die radius examined.

Importantly, Fig. 3 shows that contact between the blank and die radius in the 70° region only occurs during the transient stage. Therefore, any experimental surface degradation observed in this region can only be attributed to the transient contact pressure response (and cannot be associated with the steady-state phase).

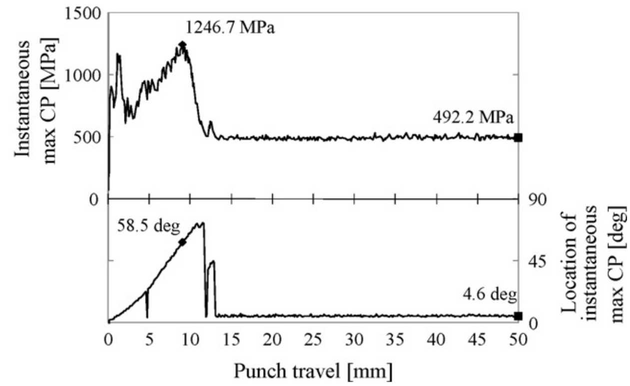

Fig. 5. Magnitude and location of instantaneous maximum contact pressure evolution on the die radius at each increment in the simulation. Peak and final contact pressure values highlighted.

These results indicate that the large pressures associated with the transient response seen in this study may be of primary significance to the wear response. Therefore the contact pressure response, and the subsequent wear response, of a typical channel forming process may not be accurately represented using a bending-under-tension test. Consequently, traditional wear tests and testing methods used for the application to sheet metal stamping dies may need to be re-evaluated.

3.4. Maximum contact pressure evolution

Due to the significance of the peak contact pressures to the tool wear performance and longevity, the evolution of the maximum contact pressure throughout the process was examined in more detail. The magnitude and location on the die radius of the maximum contact pressure was obtained at every increment in the simulation (Fig. 5). In this graph, the existence of the distinct transient and steady-state regions of the process is evident. During the entire steady-state phase, the instantaneous maximum contact pressure is approximately constant in magnitude and location. In order to determine a single value for the steady-state peak contact pressure (P_{steady}), an average value of the instantaneous maximum contact pressure in the region of 80–90% of the punch stroke was determined (i.e. between 40 and 45 mm of punch travel). This region was chosen as it provided a region of steady contact pressure, which could be used consistently for all the FE models examined in the parametric study (see Section 5). Using this method, P_{steady} was determined to be 499 MPa, occurring at 5.5° along the die radius.

The maximum contact pressure during the transient stage is consistently larger than, and up to 2.5 times that of the steady-state peak pressure. As indicated, the overall maximum pressure on the die radius (P_{max}) is 1247 MPa, occurring at an angle of 58.5° on the die radius, at the instant when the punch has traveled 9.0 mm. Hence, the overall maximum pressure is approximately three times the yield strength and almost twice the tensile strength of the blank material. A typical material utilized for the die radius inserts in the experimental setup was an AISI D2 grade cold work tool steel, with the trade name of Sverker 21, manufactured by Uddeholm Tooling [14,15]. This material was hardened to 60 HRC, resulting in a compressive yield strength of 2150 MPa [19], which is well above the maximum contact pressure predicted in the FE model; hence justifying the use of an elastic material model for the tools.

4. FE model considerations

Much care was taken in the construction and development of the FE model in order to obtain the final solution. The model development process included a systematic examination of numerous modeling inputs such as tool material model, tool mesh, relative mesh sizes at the interfaces, contact interaction definitions, etc. Due to the originality and likely significance of the results presented, this section will highlight some of the key modeling features examined, to ensure that a strong level of confidence in the predicted FE results could be obtained.

4.1. Influence of tool material elasticity

The tools are typically simplified as rigid bodies in the modeling of sheet metal forming in the literature [17,20–23]. To investigate the importance of including the tool material elasticity on the contact pressure distribution, another FE model was constructed; where the tool bodies were simplified as analytical rigid surfaces, instead of discrete elastic bodies. This allowed the additional complexity of the tool material model and the influence of the associated mesh to be ignored.

The effect of the density of the blank mesh was examined in the rigid tool model by decreasing the blank element size until a suitably converged solution was achieved, in terms of stresses, strains, contact pressure, etc. The resulting blank mesh was finely discretized, with an element side length at the surface of 0.0625 mm. Therefore, when increasing the complexity to include tool material elasticity, the baseline analytical rigid tool simulation and blank mesh was available for comparison. In order to assess the validity of the final elastic tool model and the simplified rigid tool model, another model was examined; where the modulus of elasticity of the tools was increased by an order of magnitude so that direct comparison with the rigid tool solution could be made.

Fig. 6 shows the contact pressure results obtained for the elastic, analytical rigid and artificially stiffened elastic tool models. It is evident that there is good correlation between the contact pressure response of the analytical rigid and stiffened elastic models, therefore providing a degree of confidence in the results. Furthermore, the significant effect of the tool material elasticity on the contact pressure is evident – the analytical rigid tool solution over-predicts the maximum contact pressure by 30.0%, compared to the elastic solution. Therefore it can be concluded that the elasticity of the die should be considered in the modeling process, in order to obtain an accurate contact pressure response.

4.2. Relative mesh density at die–to–blank interface

Preliminary analysis of the elastic tool solution indicated that the predicted contact pressure distribution over the die radius was sensitive to the level of mesh refinement at the interface between the blank and die radius. In particular, the ratio of the die element side length to the blank element side length at the interacting surfaces had a significant effect on the contact pressure results. It was found that if the ratio of the die–to–blank element side length at the interface was greater than or equal to one, the contact pressure response was erratic. Despite numerous mesh refinements at the interface (increasing the number of elements by up to 1600%), whilst keeping this ratio constant, the predicted contact pressure distribution over the die radius did not begin to converge to a single solution.

However, when the stated element side length ratio was reduced to less than one (i.e. the die radius element side length was shorter than the element side length at the top surface of the blank) the contact pressure results were found to be less erratic. This behavior is in disagreement with recommended conventions; where the master surface, in general, should be defined as the surface with the coarser mesh in order to avoid penetration into the slave surface [17]. Based on numerous simulations, the mesh shown in Fig. 1c was developed; ensuring that the final simulation produced a suitably converged contact pressure distribution, without using excessively large computational resources. For this mesh, the ratio of the die element side length to the blank element side length at the die radius interface was 1:2 (see Table 2).

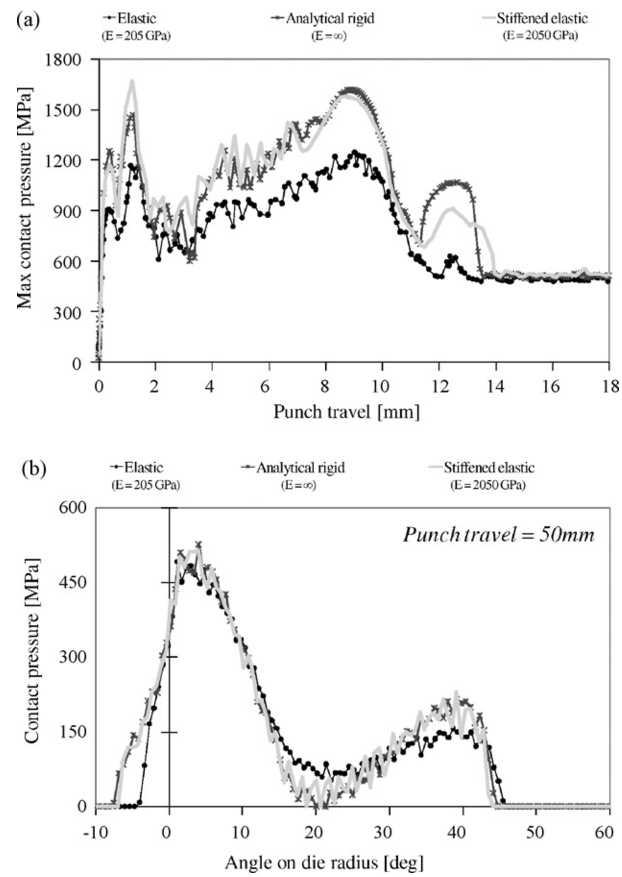

Fig. 6. Effect of tool material elasticity on (a) maximum contact pressure evolution during transient region of process, and (b) steady-state contact pressure distribution on die radius.

Fig. 7 shows the steady-state contact pressure distributions of three simulations with different die–to–blank element length ratios. In each of these simulations, the blank mesh and all other parameters were kept constant, and only the die mesh was varied in order to achieve the prescribed element length ratios. The highly

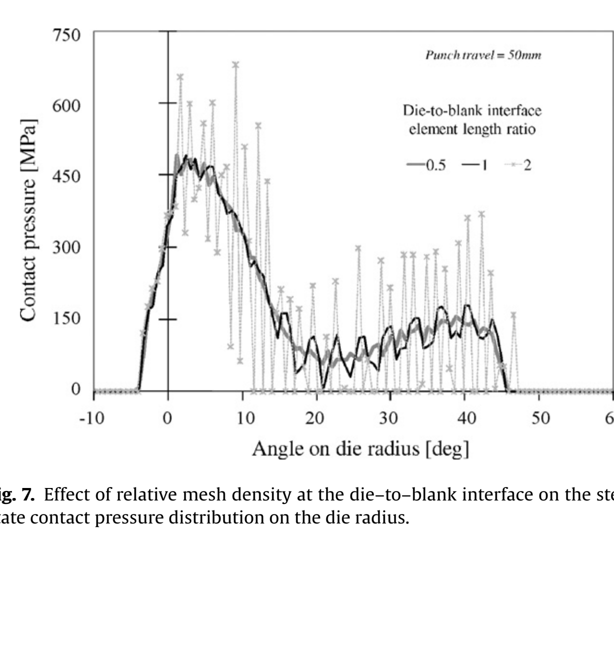

Fig. 7. Effect of relative mesh density at the die–to–blank interface on the steady-state contact pressure distribution on the die radius.

irregular contact pressure distribution predicted using an element length ratio greater than unity is apparent in Fig. 7. Conversely, it was found that the contact pressure distribution achieves a converged result for the smaller die–to–blank element ratio of 1:2. Ratios smaller than 1:2 were attempted, however these resulted in no further convergence of the contact pressure distribution, but significantly increased the computational time due to the increase in number of finite elements.

4.3. Quasi-static vs. dynamic solution

The use of the implicit FE solver ensured that a quasi-static assumption was adopted. It is well known that for analysis purposes, many sheet metal forming processes can be assumed to be quasi-static [17,20,21]. However this assumption was possibly inaccurate for this problem due to the primary interest in the initial transient stage of the forming process. In a real stamping process, the punch impacts the blank at a considerable speed. Therefore, it was speculated that the transient region may have required a dynamic simulation approach to correctly model the behavior. Consequently, an explicit model was developed in ABAQUS, based on the implicit analytic rigid tool model, in order to assess the validity of the quasi-static assumption. The rigid tool model was chosen due to its computational efficiency.

On the basis of the experimental setup, where an industrial mechanical press was used [14,15], the speed of the punch at the point where it impacts the blank was estimated. At simulated speeds of approximately 10 times the real speed, the simulation results still show good correlation with the quasi-static simulation results for the transient and steady-state regions (Fig. 8). Furthermore, the ratio of kinetic to internal energy was less than 0.5% for almost the entire simulation, thus confirming the quasi-static nature of the problem. The high level of correlation achieved for the transient contact pressure response between the two different finite element solutions, evident in Fig. 8, further validates the simulation results presented.

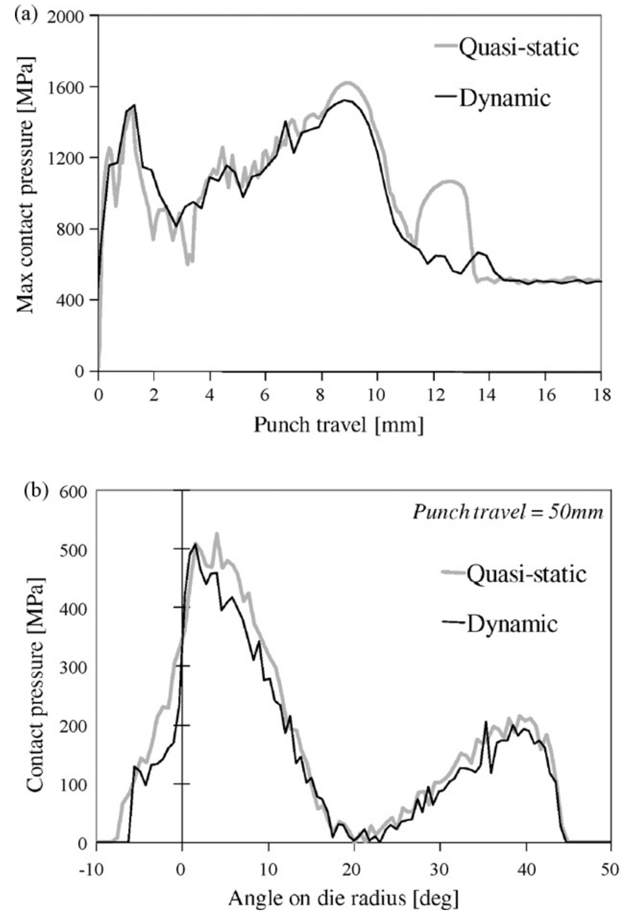

Fig. 8. Comparison between quasi-static and dynamic FE simulation results for (a) maximum contact pressure evolution during transient region of process, and (b) steady-state contact pressure distribution on die radius.

5. Parametric study

Considering the wear performance of the die during this forming process, it is perceivable that the peak contact pressures over the die radius are of particular importance. Therefore, determination of which parameters in the process have the most influence on these peak contact pressures will aid in understanding the wear response of a given tooling system. Furthermore, this will facilitate a possible reduction in tool wear, via a reduction in peak contact pressures through the optimization of the parameter values.

5.1. Parametric study description

For the FE simulation of the channel forming process, it was identified that the maximum contact pressure over the entire process (P_{max}) and the steady-state peak contact pressure (P_{steady}) are dependant on 14 parameters in the model (Eq. (2)).

$$P_{max}, P_{steady} = f(a, c, l, R_d, R_p, t, E_b, E_d, \upsilon_b, \upsilon_d, n, Y, F, \mu) \quad (2)$$

The parameters defining the geometry of the interacting tool surfaces (blank length l, blank thickness t, die radius R_d, punch width a, punch radius R_p, tool-to-sheet clearance c) were all expected to have an effect on the contact pressure. However, the effect of the overall size of the tooling (i.e. height and width) was assumed to have a negligible effect and was ignored for this analysis.

The blank material was assumed to be an isotropic elastic–plastic material in which the linear-elastic response was defined using an elastic modulus E_b and Poisson's ratio ν_b. The equivalent plastic stress–strain response of the blank material was defined using a power law equation, according to:

$$\bar{\sigma} = Y\left(1 + \frac{\bar{\varepsilon}}{\varepsilon_0}\right)^n \quad (3)$$

where $\overline{\sigma}$ is the effective stress, $\overline{\varepsilon}$ is the effective plastic strain, ε_0 is the initial yield strain, n is the work hardening exponent, and Y is the initial yield strength.

The die material was modeled using an isotropic elastic definition and thus was characterized by Poisson's ratio ν_d, and elastic modulus E_d. Considering that the contact pressure on the die radius was being analyzed, the influence of the material properties of the punch and blank holder were ignored.

The blank holder pressure was applied in the FE model using a constant force F and the friction between the tools and the blank controlled by the coefficient of friction μ. The draw depth d was not varied, as the effect of decreasing or increasing the draw depth would simply produce a smaller or larger steady-state region, respectively.

Utilizing the parameters identified in Eq. (2), a partial derivative type parametric study was undertaken. The response of the overall maximum and steady-state peak contact pressures (P_{max} and P_{steady}) were examined as each parameter was varied individually in the FE simulation, whilst all other parameters were kept constant at the original (nominal) value. The domain for each of the parameters was chosen based on the maximum and minimum values to

Table 4
Nominal, minimum and maximum values for parameters in parametric study

Parameter		Unit	Nominal	Min	Max
Punch width	a	mm	30	10	50
Tool-to-sheet clearance	c	mm	0.1	0.1	5
Blank length	l	mm	150	130	190
Die radius	R_d	mm	5	3	10
Punch radius	R_p	mm	5	3	14
Blank thickness	t	mm	2	0.5	3
Blank elastic modulus	E_b	MPa	205,000	170,000	240,000
Die elastic modulus	E_d	MPa	205,000	170,000	240,000
Blank Poisson's ratio	ν_b	–	0.3	0.25	0.35
Die Poisson's ratio	ν_d	–	0.3	0.25	0.35
Blank hardening exponent	n	–	0.15	0.1	0.2
Blank yield strength	Y	MPa	400	300	700
Blank holder force	F	N	450	112.5	900
Initial average holder pressure	P_h	MPa	8.5	2.1	17.0
Friction coefficient	μ	–	0.15	0.05	0.3

be reasonably expected in the real forming process of steel sheet. In some cases, the allowable domain was constrained by the physical geometry of the original process setup. For example, the maximum value of the die radius was limited by the final part flange length; the maximum value of the punch radius was limited by the punch width; etc. For each parameter, 5 or 6 values were chosen within the defined domains, to allow the first order effect on the maximum and steady-state peak contact pressures to be determined in detail throughout the domain. Therefore, a total of 64 FE models were constructed and analyzed, in order to conduct the parametric study on the 14 parameters identified. Table 4 details the nominal values and domains used for each of the parameters.

In many cases, the parametric study involved modification of the geometry and consequently the mesh of the tools or blank. In each of these cases, care was taken to ensure that the element lengths at the interacting surfaces were kept approximately constant, due to the previously determined sensitivity of the contact pressure to the mesh.

5.2. Parametric study results

The individual effect of each of the parameters on the maximum and steady-state peak contact pressures are presented in the 14 graphs of Fig. 9. The abscissa in each graph denotes the value of the parameter being varied and, as such, each point represents a different FE model. The ordinate indicates the percentage change in P_{max} and P_{steady} from the respective nominal values, allowing direct comparison between the behavior of the maximum contact pressure and the steady-state peak contact pressure. Therefore, the point at which each of the curves intersects the x-axis represents the nominal value of contact pressure, as determined from the nominal FE simulation described in Sections 3 and 4.

As stated earlier, P_{steady} was calculated by taking an average of the values of instantaneous maximum contact pressure between 40 and 45 mm of punch travel, during the simulation results history. Therefore the standard deviation associated with P_{steady} was calculated for each of the 64 simulations, and was found to be typically between 2 and 4%. Due to this relatively small standard deviation, error bars could not be clearly indicated on the graphs of Fig. 9, and were therefore excluded. Error bars are not required for P_{max}, due to its singular nature.

The individual responses of P_{max} and P_{steady} to each of the parameters investigated (Fig. 9) can be used to provide an insight into which factors in the real forming process are likely to affect tool wear. Therefore, a discussion of each of the responses which display a significant influence on the peak contact pressures will be provided. However, a detailed explanation describing the reason for the responses is beyond the scope of this investigation.

5.3. Effect of die radius, R_d

The die radius parameter has a strong inverse effect on both P_{max} and P_{steady}. At the lower values of die radius in particular, the response is highly non-linear; with both P_{max} and P_{steady} showing a rapid increase as the die radius is decreased from the nominal value. However, the effect of the die radius is more pronounced for P_{max}. In all cases, the percentage change in P_{max} from the nominal is more than twice that for P_{steady}. These results indicate that the peak contact pressure (and by association, tool wear), can be reduced by choosing the largest feasible die radius.

5.4. Effect of blank thickness, t

P_{max} and P_{steady} exhibit a large and approximately linear response to changing blank thickness, with the percentage change from the nominal values very similar in both cases. The behavior of the peak contact pressure variables, with respect to blank thickness and die radius, provide an insight into a traditional rule-of-thumb often adopted in the sheet metal forming industry, where the severity of a drawing or bending operation is assessed by the bend ratio ρ/t. This is the ratio of the radius of curvature formed by the mid-plane of the blank ρ to the thickness of the blank t. Utilizing the results of the simulations which varied die radius and blank thickness, it is possible to plot the effect of the bend ratio (Fig. 10). It is evident from Fig. 10 that decreasing the bend ratio has a significant effect on the severity of the maximum tribological stresses experienced over the die radius. Furthermore, there are two instances where two separate simulations have the same value of bend ratio ($\rho/t=2.5$ and $\rho/t=5.5$), but with differing values of die radius and blank thickness. In each case, the values of P_{max} and P_{steady} were approximately the same for the equivalent bend ratios. Therefore, it can be concluded that the bend ratio is a useful index to judge the severity, in relative terms, of the sheet metal forming operation on the die tooling.

5.5. Effect of blank material yield strength, Y

The peak contact pressure variables display an approximately linear response to the blank material yield strength parameter, with the percentage change from the nominal values for both P_{max} and P_{steady} being very similar. Comparison between the response

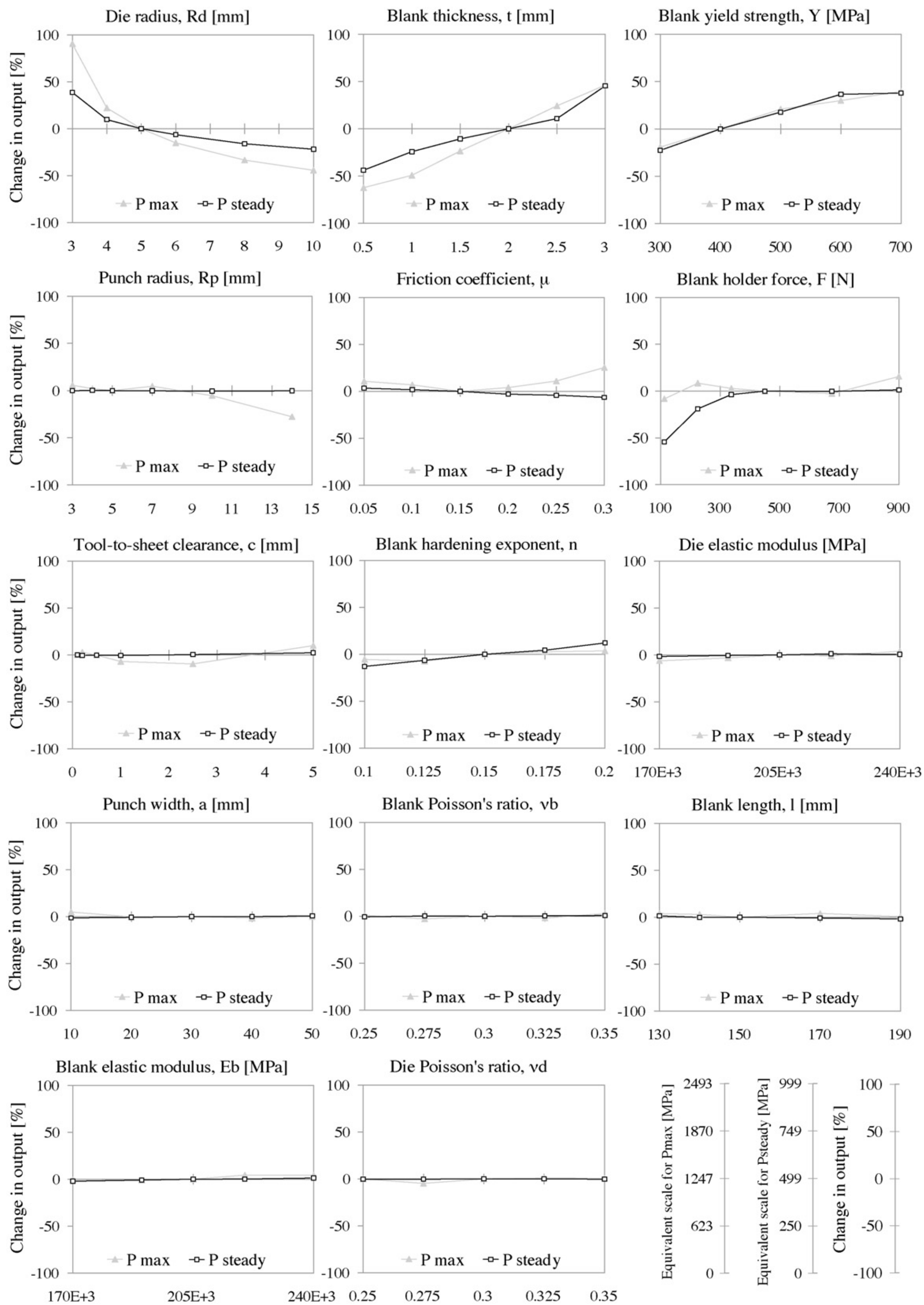

Fig. 9. Results of the parametric study showing the percentage change in maximum and steady-state peak contact pressures for each of the parameters examined.

to the blank thickness and blank yield strength parameters in Fig. 9 reveals that the behavior of $P_{\max}$ and P_{steady} are quite similar in both cases. This fact is logical; as it can be expected that increasing the resistance to deformation (i.e. stiffness) of the blank, through the increase of either thickness or yield strength, will result in increased contact pressures over the die radius. This result has direct implications on the tool wear associated with introducing high strength steels to stamping.

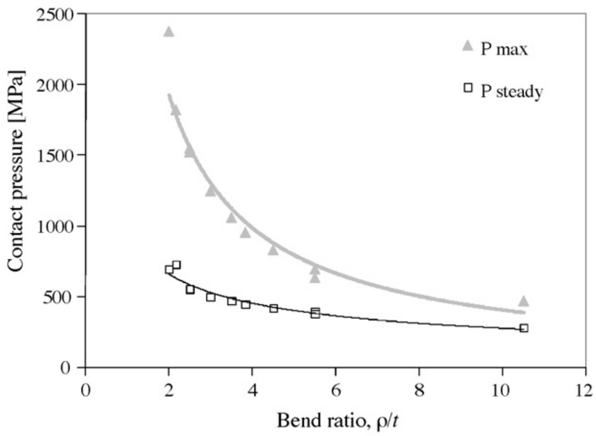

Fig. 10. Effect of bend ratio on the maximum and steady-state peak contact pressures (solid lines represent fitted curves using a power law relation).

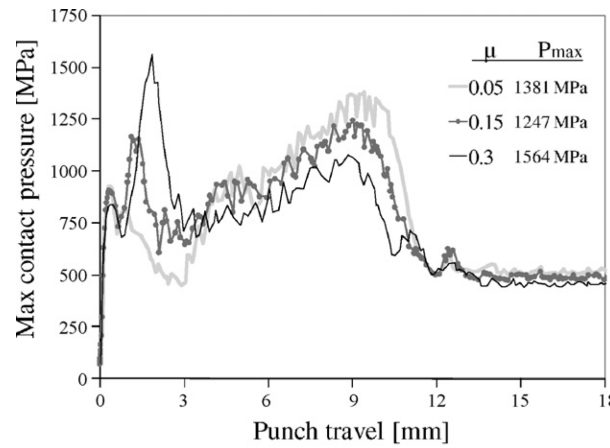

Fig. 11. Maximum contact pressure evolution on the die radius during the transient portion of the process for differing values of friction coefficient.

5.6. *Effect of punch radius, R_p*

Changing the punch radius produces distinctly different responses between P_{max} and P_{steady}. The behavior of P_{steady} is approximately constant at all values of punch radius, with less than a one percent change from the nominal value in all cases. Considering that the standard deviation associated with calculating P_{steady} is between 2 and 4% in all cases, it can be concluded that the punch radius has an insignificant effect on P_{steady} for the range of values examined. Conversely, the punch radius has a significant inverse effect on P_{max}, for the larger radii in particular. For example, at the maximum value of punch radius (14 mm), P_{max} decreases by 27.7% from the nominal value. Therefore, it is evident that the punch radius has an influence on the transient contact pressure response, but has little or no effect on the steady-state contact pressure response.

5.7. *Effect of friction coefficient, μ*

The value of the friction coefficient also causes differing trends between the responses of P_{max} and P_{steady}. P_{steady} exhibits a small and approximately linear inverse effect; where the range, between the maximum and minimum change from nominal, is 9.8%. This is larger than two standard deviations, and therefore can be considered statistically significant, despite the effect being very small.

The effect of friction coefficient on P_{max} is larger, but highly non-linear and non-monotonic. Since the friction coefficient is the first parameter to be discussed with a significant non-monotonic response, a more detailed examination of the results will be presented to justify that such a response is not due to an unreliable result. However, such an analysis for all the other parameters is beyond the scope and objectives of this investigation, and therefore will be not be included.

Fig. 11 can be used to explain the occurrence of this non-monotonic response. This graph shows the evolution of the maximum contact pressure for three of the FE models with different friction coefficients specified (the minimum, nominal and maximum values used in the parametric study). It is evident that there are two significant peaks in the maximum contact pressure evolution throughout the stroke for each of the models. Thus, the behavior of these two peaks, which do not necessarily show the same response in all cases, directly effects the value of the overall peak contact pressure (P_{max}) obtained. In this case, the first peak increases with friction coefficient, whilst the second peak decreases, causing the non-monotonic response in P_{max}. Most of the models examined in this parametric study exhibit this two-peak maximum contact pressure evolution curve during the transient stage of the process. Therefore, this type of opposing behavior between the two peaks is often the reason behind any non-monotonic response for P_{max}.

It is worth noting that although the friction coefficient has a relatively small effect on the maximum contact pressures, it is expected that it will have a more significant effect on the tool wear due to the additional shear forces which will occur at the interacting surfaces.

5.8. *Effect of blank holder force, F*

The blank holder force also causes a non-monotonic response from P_{max}. Despite the fluctuating behavior, the overall effect of blank holder force on P_{max} is relatively small. Interestingly, the minimum and maximum values of blank holder force correspond to the minimum and maximum values for P_{max} – representing −8.4 and 15.5% change from nominal, respectively. This aspect may indicate a small positive response from P_{max} to increasing blank holder force.

The effect of blank holder force on P_{steady} is larger; however there is a distinct two-stage response for the domain examined. Beginning from the minimum value of blank holder force of 112.5 N, P_{steady} shows a large increase as the blank holder force is increased. However, beyond the nominal value of blank holder force of 450 N, P_{steady} exhibits an approximately constant response. Examination of the deformed shape of the blank over the die radius during the steady-state region, for the models with minimum and nominal blank holder force, provides an explanation of the two-stage response (Fig. 12). This shows that for the model with minimum blank holder force, there is insufficient clamping force to keep the blank holder closed, causing a gap to exist between the blank and die at the beginning of the die radius. Consequently, the radius of curvature of the blank is effectively increased, resulting in a reduction in P_{steady}, as seen for models with larger die radii (Section 5.3). This effect is not seen in the models with blank holder force equal to or greater than the nominal value; where there is sufficient clamping force to ensure that the shape of the blank closely conforms to the die radius (Fig. 12b). As such, the actual effect of blank holder force on P_{steady} is negligible, as the real process should provide sufficient clamping to keep the blank holder closed.

5.9. *Effect of tool-to-sheet clearance, c*

In order to avoid the possibility of creating an ironing process, the nominal tool clearance of 0.1 mm was defined as the minimum

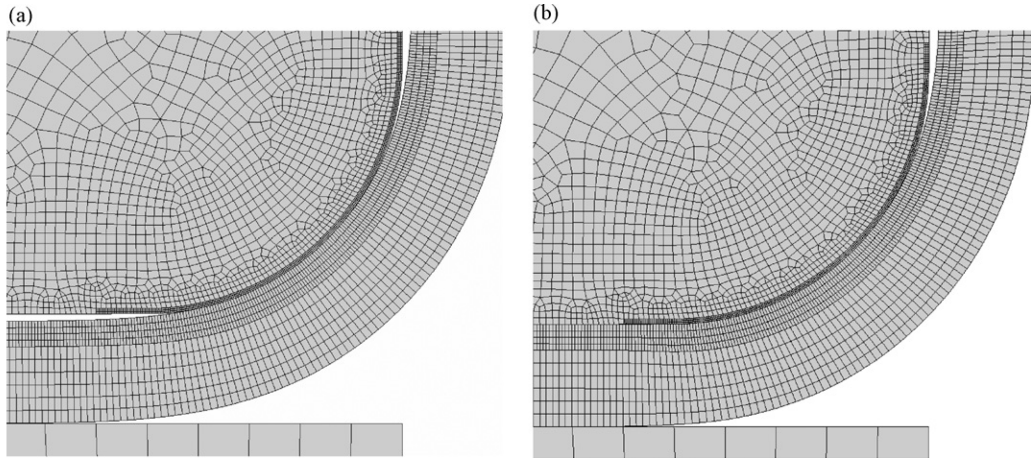

Fig. 12. Deformed plot of die radius region at full punch stroke for models with blank holder force of (a) 112.5 N and (b) 450 N.

value. Increasing the tool clearance above the nominal value had a negligible effect on P_{steady}. Conversely, the value of tool-to-sheet clearance has a small and non-monotonic influence on P_{max}.

These results indicate that, in a similar trend to the effect of punch radius, the tool-to-sheet clearance has a notable influence on the transient contact pressure response, but has little or no effect on the steady-state contact pressure response. It is evident that the transient contact pressure response is affected by the way in which the blank is forced to conform to the die radius as the punch moves upwards and deforms the blank. Changing the punch radius and tool-to-sheet clearance each have the effect of altering this transient 'wrapping' stage, thus influencing the transient response and affecting P_{max}. However, as the punch moves further upwards and the process progresses into the steady-state portion, the angle of wrap of the blank will be similar; where the side-wall of the formed component will be almost vertical in all cases. Consequently, the steady-state contact pressure responses and the associated values of P_{steady} will be relatively unchanged.

5.10. Effect of blank material hardening exponent, n

The value of the blank material hardening exponent has a small positive influence on both P_{max} and P_{steady}. However, in this case, the percentage change from the nominal value of P_{steady} is larger than that for P_{max}.

Interestingly, the blank material hardening exponent has a smaller influence on the peak contact pressures than the blank material yield strength for the domains examined (Section 5.5). In line with the conclusions drawn in Section 5.5 – where an increase in the blank's resistance to deformation results in an increase in peak contact pressure – it was expected that the hardening exponent would have a similarly significant affect on the contact pressure. The smaller influence of hardening exponent can be explained by examining the resulting blank material ultimate tensile strength (UTS) in each case. Due to the material law used (Eq. (3)) and the domains examined (Table 4), changing the yield strength results in a range of UTS values from 494 to 1154 MPa. However, changing the n-value corresponds to a smaller range of UTS values, from 536 to 824 MPa. Therefore, it is likely that the blank material UTS may provide a more useful relationship to the peak contact pressures than either hardening exponent or yield strength.

Utilizing the results of the simulations which varied blank hardening exponent and yield strength, it is possible to plot the effect of the blank material UTS (Fig. 13). It is evident from Fig. 13 that increasing the UTS has strong linear effect on both P_{max} and P_{steady}. Due to the large amount of plastic deformation experienced by the blank during the stamping process, this result further illustrates that an increase in the blank's resistance to deformation will cause an increase in the peak contact pressure experienced at the die radius. Considering the significant strain-hardening behavior of new generation high strength steels, this result demonstrates the likely increase in tool wear associated with these new sheet materials.

5.11. Effect of die material elastic modulus, E_d

The die material elastic modulus does not have a significant effect on the value of P_{steady}. The change from the nominal value of P_{steady} is less than ±2%. However, the die elastic modulus does have a small positive effect on P_{max}; where the range, between the maximum and minimum change from nominal, is 10.1%. For the domain examined, it is evident that the stiffness of the die material had very little effect on the peak contact pressures examined. This is primarily because the range examined is small, in an attempt to be representative of the maximum domain for the modulus of steel and iron only. However, it was observed earlier (Section 4.1) that the effect of stiffness is more significant when the stiffness is increased dramatically (i.e. changing from elastic to rigid), thus justifying the approach to model the tools using an elastic material model.

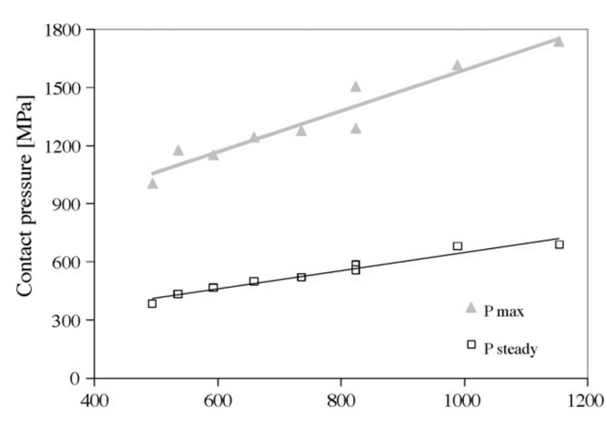

Fig. 13. Effect of blank material ultimate tensile strength (UTS) on the maximum and steady-state peak contact pressures (solid lines represent a linear curve fit).

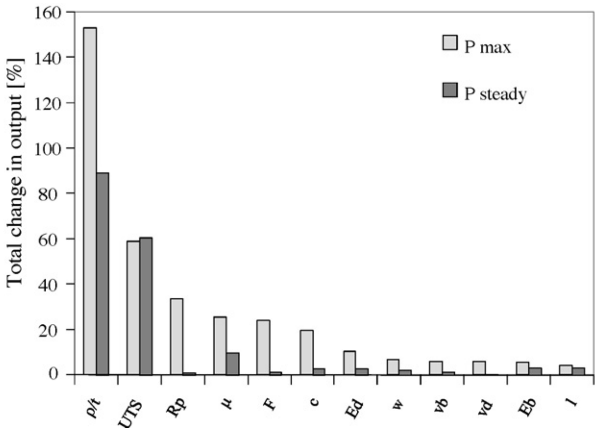

Fig. 14. Summary of the effect of each of the input parameters on the maximum and steady-state peak contact pressures.

5.12. Other parameters

The other parameters examined as part of the parametric study had little or no effect of P_{max} and P_{steady}. These parameters were punch width, blank material Poisson's ratio, blank length, blank material elastic modulus, and die material Poisson's ratio. The average magnitude of change from the nominal values of P_{max} and P_{steady} for the domain of each of these parameters is less than 2.5%.

5.13. Summary of parametric study

In order to clearly summarize which parameters in the study had the most effect on the maximum and steady-state peak contact pressures, the percentage total change in output for each parameter was calculated (Fig. 14). This value represents the range (i.e. maximum minus minimum) of P_{max} values and P_{steady} values achieved when varying each parameter within the specified domain, expressed as a percentage of the respective nominal values. The parameters in Fig. 14 are ordered in terms of the most influence on P_{max}. The influence of the low blank holder force values, where the force was insufficient to keep the blank holder closed during the steady state, was removed. Additionally, due to the identified relationships identified, the effects of die radius and sheet thickness are expressed in the bend ratio parameter, and the effects of the blank material hardening exponent and yield strength are summarized with the UTS parameter.

Fig. 14 highlights the differing responses of P_{max} and P_{steady} to the input parameters. Nevertheless, the two most influential parameters on P_{max} (bend ratio and blank material UTS) also have the most effect on P_{steady}. It is evident that the strong influence on the steady and transient contact pressure distributions arises from the direct influence of each of these parameters on the amount of bending, or the resistance to bending, of the blank over the radius.

It is interesting to note that the main process parameters, friction coefficient and blank holder force, have only a very small effect on both P_{max} and P_{steady}. The fact that these process parameters have only a small effect may initially seem counter intuitive, as both these parameters influence the amount of tension that is developed in the sheet. Therefore it would be expected that if the sheet tension increases, the force on the die radius and thus the peak contact pressures should increase proportionally. However, this is not the case, and it appears that the peak contact pressures are influenced to a greater extent by the degree of bending that occurs over the die radius and the resistance to bending produced by the blank.

Other geometrical parameters (punch radius and tool-to-sheet clearance) had notable effects on P_{max}, but not on P_{steady}. This result highlights that these parameters influence the transient portion of the process, through the modification of the geometric/loading conditions that occur as the blank is initially formed over the die radius, but have little influence on the steady-state response. Therefore, if the maximum contact pressure P_{max} is of primary significance to tool wear, such geometric parameters may possibly be optimized to improve the wear response of a given stamping process.

6. Summary

The evolution and distribution of contact pressure over the die radius, throughout the duration of a channel forming process, was determined using FE analysis. For the majority of the process, a steady-state contact pressure distribution occurred over the die radius. This distribution was characterized by a smooth two-peak response; which qualitatively compared well with experimental and numerical results presented in the literature for bending-under-tension processes.

It was found that a transient response occurs during the initial stages of the forming process, not previously seen in the literature. This part of the process was characterized by highly localized and severe contact conditions, resulting in contact pressures exceeding double the steady-state peak pressure. Considering the mechanisms of wear in sliding contact, these results suggest that the transient response identified and described may be of primary significance to the tool wear response for a channel forming process. This result has been validated by laboratory-based channel forming wear tests, which showed that the transient contact pressure region corresponded to a severe galling wear mechanism. Therefore, it was speculated that current bending-under-tension wear test results may not be entirely applicable to the wear of stamping dies.

Through additional numerical analysis, it was concluded that the elasticity of the die should be considered in the modeling process, in order to obtain an accurate contact pressure response. It was also found that the dynamic effect for this problem can be neglected; with the quasi-static model accurately simulating the contact pressure response.

A parametric study was conducted to assess the influence of the input parameters to the transient and steady-state peak contact pressures. It was found that the major process parameters in the sheet metal forming process, friction coefficient and blank holder force, had only a minor influence. Conversely, the bend ratio and the blank material ultimate tensile strength had the most influence on the transient and steady-state peak contact pressures. This demonstrated that the bend ratio provided a useful index to judge the severity of the forming operation. The result of the parametric study also highlighted that modification of the stiffness of the blank (i.e. through yield strength, hardening exponent or thickness changes), has a similarly strong influence on the contact pressure experienced on the die radius. Therefore, the trend towards higher strength steels in the automotive industry may need to be offset by an increase in the die radius to ensure that tool life of draw dies can be maintained.

Acknowledgements

This research was supported by Ford Motor Company USA, Ford of Australia, Volvo Cars Sweden, an Australian Research Council Linkage Project (LP0776913), and by an award under the Merit Allocation Scheme on the National Facility of the Australian Partnership for Advanced Computing. The authors extend their gratitude to Professor Peter Hodgson from Deakin University and Professor John Duncan from Auckland University for their support.

References

[1] R.G. Bayer, Engineering Design for Wear, Marcel Dekker, New York, 2004.
[2] H.C. Meng, K.C. Ludema, Wear models and predictive equations: their form and content, Wear 181–183 (1995) 443–457.
[3] S.K. Rhee, Wear equation for polymers sliding against metal surfaces, Wear 16 (1970) 431–445.
[4] R.G. Bayer, A general model for sliding wear in electrical contacts, Wear 162–164 (1993) 913–918.
[5] J.F. Archard, Contact, Rubbing of flat surfaces, Journal of Applied Physics 24 (1953) 981–988.
[6] S.M. Hsu, M.C. Shen, A.W. Ruff, Wear prediction for metals, Tribology International 30 (1997) 377–383.
[7] W. Yan, E.P. Busso, N.P. O'Dowd, A micromechanics investigation of sliding wear in coated components, Proceedings of the Royal Society A: Mathematical, Physical and Engineering Sciences 456 (2000) 2387–2407.
[8] W. Yan, Theoretical investigation of wear-resistance mechanism of superelastic shape memory alloy NiTi, Materials Science and Engineering: A 427 (2006) 348–355.
[9] C. Boher, et al., Wear behaviour on the radius portion of a die in deep-drawing: Identification, localisation and evolution of the surface damage, Wear 259 (2005) 1097–1108.
[10] G.J. Coubrough, M.J. Alinger, C.J. Van Tyne, Angle of contact between sheet and die during stretch-bend deformation as determined on the bending-under-tension friction test system, Journal of Materials Processing Technology 130–131 (2002) 69–75.
[11] M. Eriksen, The influence of die geometry on tool wear in deep drawing, Wear 207 (1997) 10–15.
[12] K. Hanaki, K. Kato, Pressure peak in bending and unbending process, Advanced Technology of Plasticity 1 (1984) 581–586.
[13] D. Hortig, D. Schmoeckel, Analysis of local loads on the draw die profile with regard to wear using the FEM and experimental investigations, Journal of Materials Processing Technology 115 (2001) 153–158.
[14] O. Sandberg, et al., Characterisation of tool wear in stamping of EHS and UHS steel sheets, Proc. International Conference on Recent Advances in Manufacture & Use of Tools & Dies and Stamping of Steel Sheets, Olofström, Sweden, 2004, pp. 151–170.
[15] T. Skåre, F. Krantz, Wear and frictional behaviour of high strength steel in stamping monitored by acoustic emission technique, Wear 255 (2003) 1471–1479.
[16] S.A. Asgari, et al., Statistical analysis of finite element modeling in sheet metal forming and springback analysis, Journal of Materials Processing Technology 203 (2008) 129–136.
[17] ABAQUS Inc., ABAQUS Version 6.5 Documentation, Dassault Systems, Providence, RI 02909, USA, 2004.
[18] M. Pereira, W. Yan, B.F. Rolfe, Contact pressure and wear in sheet metal forming—an FEM analysis, Proc. International Conference and Exhibition on Structural Integrity and Failure, Sydney, Australia, pp. 73–77.
[19] Uddeholm Tooling AB, Sverker 21 Product Brochure, Uddeholm Tooling AB, Mölndal, Sweden, 2003.
[20] N. Rebelo, J.C. Nagtegaal, H.D. Hibbit, Finite element analysis of sheet forming processes, International Journal for Numerical Methods in Engineering 30 (1990) 1739–1758.
[21] S.C. Tang, Trends on Simulation of Sheet Metal Forming Processes, SAE Transactions: Journal of Materials & Manufacturing 109 (2000) 523–530.
[22] A.E. Tekkaya, State-of-the-art of simulation of sheet metal forming, Journal of Materials Processing Technology 103 (2000) 14–22.
[23] M. Tisza, Numerical modelling and simulation in sheet metal forming, Journal of Materials Processing Technology 151 (2004) 58–62.